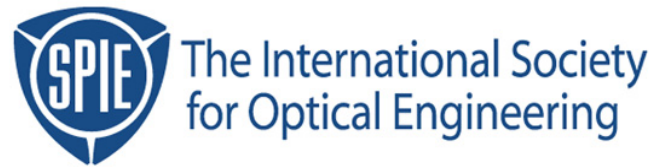


Copyright 2000 by the Society of Photo-Optical Instrumentation Engineers.



This paper was published in the proceedings of
Photomask and X-Ray Mask Technology VII
SPIE Vol. 4066, pp. 160-171.

It is made available as an electronic reprint with permission of SPIE.

One print or electronic copy may be made for personal use only. Systematic or multiple reproduction, distribution to multiple locations via electronic or other means, duplication of any material in this paper for a fee or for commercial purposes, or modification of the content of the paper are prohibited.

Lithography Performance of Contact Holes — Part I. Optimization of Pattern Fidelity Using MPG and MPG-II

Suzanne Weaver, Maiying Lu, Jan Chabala, Dinh Ton, Charles Sauer, and Chris Mack*

Etec Systems, Inc., 26460 Corporate Avenue, Hayward, CA 94545 USA
Phone: (510) 780-3703; fax: (510) 887-2870; e-mail: sweaver@etec.com

*FINLE Technologies, 8834 Capital of Texas Highway, Suite 301, Austin, TX 78759 USA
Phone: (512) 327-3781; fax: (512) 327-1510; e-mail: chris_mack@finle.com

ABSTRACT

Proximity effects make optimizing the pattern fidelity of contact holes one of the most challenging lithographic tasks in maskmaking. This paper examines the exposure and process parameters that influence the pattern fidelity of contact holes on a photomask from both a modeling and an experimental approach. To optimize contact critical dimension (CD) uniformity and corner rounding, a range of exposure and process variables is examined. These variables include MEBES[®] writing strategy (which is multipass gray, also known as *MPG*, and *MPG-II*), input address, spot size, development time, and data bias. ProBEAM/3D, an electron-beam (e-beam) modeling software program, is used to model contact hole performance, and the results are verified with a design of experiments protocol using the same variables as in the simulation study. A simultaneous optimization of these parameters is instructive in matching the appropriate writing strategy and technology node with the desired quality of the contact hole.

Keywords: MEBES, MPG, MPG-II, ProBEAM/3D, contact holes

1. INTRODUCTION

Printing contact holes is one of the most challenging tasks in mask lithography. As feature sizes continue to shrink, this challenge becomes even greater as proximity effects begin to affect pattern fidelity. Contact patterns are being printed today in which the contact spacing or pitch is within the backscatter radius at 10 keV. This trend strongly suggests that proximity effect correction (PEC) is necessary for the best critical dimension (CD) results. In addition to proximity correction, other exposure and process parameters may exist that can be optimized to improve contact lithography. Writing strategy is one such exposure parameter, and Etec Systems has recently introduced a new multipass writing strategy — *MPG-II*.¹ It is instructive to examine this strategy and to compare it with *MPG*, the writing strategy used earlier, to quantify any differences between the two strategies.² Given the wide range of input addresses, spot sizes, and data biases that are used in the industry for printing of contact holes, a determination of the acceptable process window and applications space for contact holes is warranted.

The purpose of this series of experiments is to evaluate contact lithographic performance dependence on writing strategy, input address, spot size, data bias, and development time. The evaluation is performed through simulation as well as experiment. The goal is to define the optimum exposure and process conditions for each writing strategy and to compare the lithographic merits of both strategies. In addition, the comparison of experimental data to simulation will gauge the effectiveness of simulation as a tool for process development and system characterization.

2. DESCRIPTION OF EXPERIMENT

An experimental matrix was defined to examine contact performance with *MPG* and *MPG-II* writing strategies. The variables are writing strategy, input address, spot size, data bias, and development time.

A distinct set of exposure parameters was chosen for each writing strategy according to its limits. Tables 1 and 2 outline the factor space probed for simulation and experiment, respectively.

Three contact feature sizes were studied to determine the effects of data bias on contact lithography. The design included contacts with 540 nm, 630 nm, and 720 nm dimensions. In the experiment, the target CD for these features was 720 nm*. The 540 nm feature, therefore, represents a 180 nm biased contact; the 630 nm design represents a 90 nm bias; and the 720 nm contact, the 0 bias case. For simulation, a slightly different set of biases was used: 0 nm, 100 nm, and 200 nm were chosen, such that target CDs varied slightly compared to the experimental set.

Table 1. Simulation factor space.

Factor	Units	MPG			MPG-II		
		Low	Middle	High	Low	Middle	High
Dev. time	sec	167	196	236	164	194	234
Spot size	nm	80	160	240	80	140	200
Bias	nm	0	100	200	0	100	200
Address	nm	15	30	45	5	10	15

Table 2. Experimental factor space.

Factor	Units	MPG			MPG-II		
		Low	Middle	High	Low	Middle	High
Dev. time	sec	200	240	280	200	240	280
Spot size	nm	80	160	240	80	140	200
Bias	nm	0	90	180	0	90	180
Address	nm	15	30	45	5	10	15

A range of development times was chosen to span the entire factor space so that each bias case would have at least one contact feature resolved. The range and magnitude of these times varied slightly between simulation and experiment. This is expected because the simulation does not model the etch process and the resist parameter file it uses is determined experimentally. In addition, the 630 nm feature was always used for targeting in the simulation, regardless of bias. For the experiment, the target CD was always 720 nm, so that in the case of the 90 nm bias, the feature designed at 630 nm was measured.

A commercial statistical analysis software package, Design-Expert 5, was used to analyze the simulation and experimental data. A central-composite design was used to map the entire parameter space, while minimizing the number of experiments.³ Analysis was performed using a quadratic fit to the data in all cases. Each writing strategy was run as a separate experiment. Twenty-five data samples were used for both the simulation and the experiment of each writing strategy. For simulation, the output parameters were mean-to-target CD and sidewall angle. For experiment, the responses were mean-to-target CD and area fill. An additional simulation was run to quantify $\Delta\text{CD}/\%\Delta\text{dose}$, the change in CD per percent change in dose. This required 15 data samples for each writing mode and excluded development time as a variable.

3. SIMULATION PARAMETERS

ProBEAM/3D (v 5.1q)⁴ software was used to model the experiment. The input required to generate the simulation includes a resist parameter file, the exposure conditions (beam energy, beam size, dose, and substrate material), and a pattern image defined by exposed pixels.

* To prevent grid snapping for the 10-nm and 30-nm input addresses, the design CD for the 90 nm biased feature was changed from 630 nm. The mean-to-target evaluation for simulation and experiment was determined according the actual design size in all cases. For example, for a 30-nm input address, the 90 nm biased contact was designed at 600 nm with a corresponding target CD of 690 nm.

Table 3 provides a list of the dissolution rate parameters for three development processes and is representative of the information required in the resist parameter file for ProBEAM/3D. A standard PBS process, a ZED 500 developer process used with the MEBES 5000⁵ system, and a ZED 750 process used with the MEBES 5500 system,⁶ are shown.

Table 3. Dissolution rate parameters for MEBES 5000 and 5500 processes.

Dissolution Rate Parameter	Symbol	Processes		
		MEBES 5000	MEBES 5500	Standard PBS
Developer		ZED 500	ZED 750	MnPK/MIAK
Maximum develop rate (nm/sec)	R_{max}	13.1	12.0	32.9
Minimum develop rate (nm/sec)	R_{min}	0.188	0.060	2.210
Threshold concentration	m_{th}	0.45	0.45	-1000.00
Dissolution selectivity	n	7.27	7.50	2.22
Exposure rate constant (cm ³ /J)	C	0.0096	0.0080	0.0050

Table 3 shows that the two ZEP processes are very similar in their dissolution rates, with the MEBES 5500 process displaying a slightly higher contrast. The PBS and MEBES 5000 parameters are included for reference only. For the simulations in this paper, only the MEBES 5500 parameters were used.

With the given parameter file, a Monte Carlo simulation was run using 100,000 electrons of 10 KeV energy traversed through 400 nm of ZEP 7000 resist and 100 nm of chromium on a quartz substrate. The energy distribution of the Monte Carlo was binned arithmetically on a 2D grid. The energy distribution was then convolved with a Gaussian profile to produce a simulated interaction of a Gaussian beam of electrons on the photoresist. The images of the energy placed on the resist were then convolved further with the pattern images to produce 2D aerial images. The aerial images were processed through the Original Mack resist development model.⁷ The Original Mack model was used to better simulate the resist contrast curve obtained experimentally. This model gave the x-z profiles or cross-section images of the resist profile. The profile CD sizes and resist wall angles were measured using the ProBEAM/3D Metrology raw method at a 30% set point.⁸ The 30% set point used in the CD measurement was chosen to accurately depict the resist profile after chrome etch.

The development times were chosen such that the 630 nm contact hole exposed with a 45 nm input address and MPG, and the same size contact exposed at a 15 nm input address with MPG-II, developed to the target CD size. For example, for the exposure with MPG and 100 nm biasing, the development time was chosen so that the 630 nm contact with a 45 nm input address developed to 730 nm.

4. SIMULATION RESULTS

The change in CD with respect to percent change in dose ($\Delta CD/\% \Delta dose$) is a useful parameter for gauging process latitude. A low value of $\Delta CD/\% \Delta dose$ indicates greater process latitude in that the process is fairly insensitive to minor fluctuations in dose and develop time.

Simulation results for $\Delta CD/\% \Delta dose$ are similar for MPG and MPG-II, as shown in Figures 1 and 2, respectively. Figures 1 and 2 are perturbation plots generated by the analysis software. Perturbation plots show the effect of changing one factor while holding the rest constant. This is useful because variables can be examined. Figures 1 and 2 show that $\Delta CD/\% \Delta dose$ (nm) is most sensitive to spot size, with some dependence on bias and minimal influence from the input address. These figures also indicate that MPG and MPG-II have similar lithographic responses to the variables tested.

Figure 1. $\Delta CD/\Delta\%dose$ for MPG.

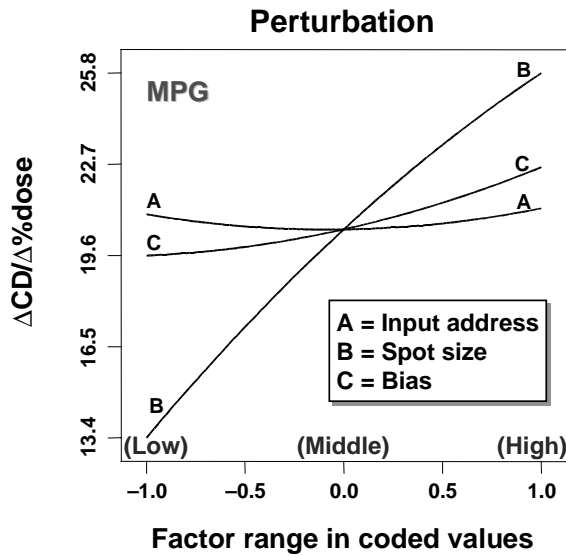
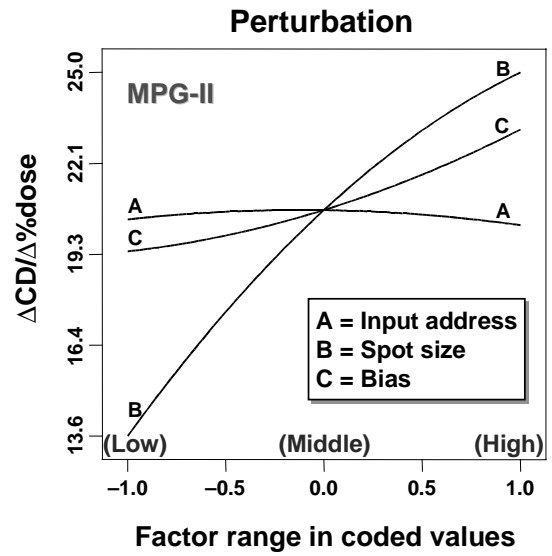


Figure 2. $\Delta CD/\Delta\%dose$ for MPG-II.



Figures 3 and 4 are contour plots of $\Delta CD/\Delta\%dose$ for both writing strategies as a function of spot size and bias; the input address is constant in both cases, since $\Delta CD/\Delta\%dose$ is fairly insensitive to the input address. The input address size is fixed at the center points of the experiment, 30 nm for MPG, and 10 nm for MPG-II.

Figure 3. $\Delta CD/\Delta\%dose$ as a function of spot size and bias — MPG, 30 nm input address.

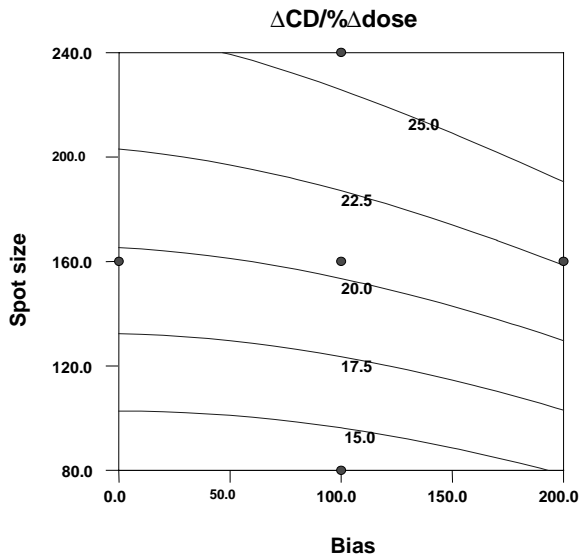
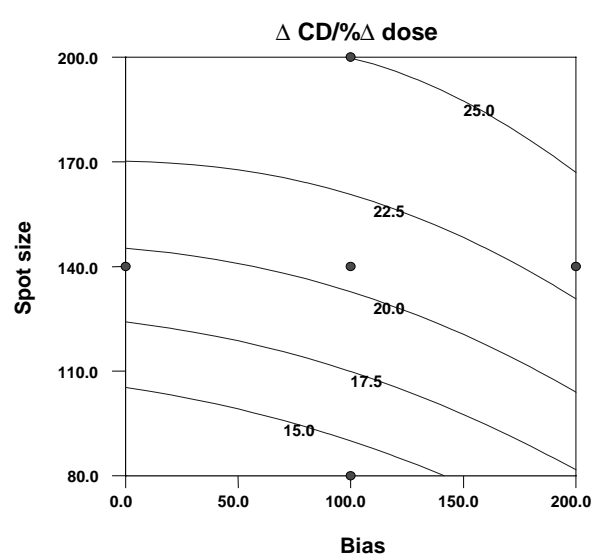


Figure 4. $\Delta CD/\Delta\%dose$ as a function of spot size and bias — MPG-II, 10 nm input address.



Figures 5 and 6 are simulation contours of the contact sidewall angle as a function of spot size and bias for MPG and MPG-II, respectively. The contours show that the sidewall angle degrades with increased spot size and bias. The sidewall angle response to the variables supports the $\Delta CD/\Delta\%dose$ response to these same variables. This demonstrates that shallower sidewall slope induces a larger change in CD with respect to percent change in dose than a steeper slope.

Figure 5. Sidewall angle as a function of spot size and bias — MPG, 15 nm input address, 167 sec development time.

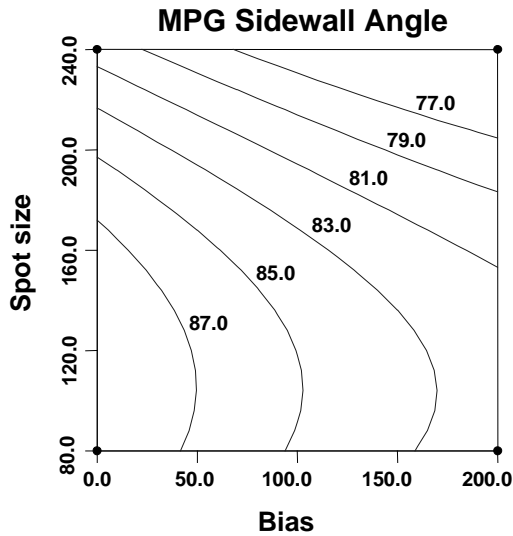
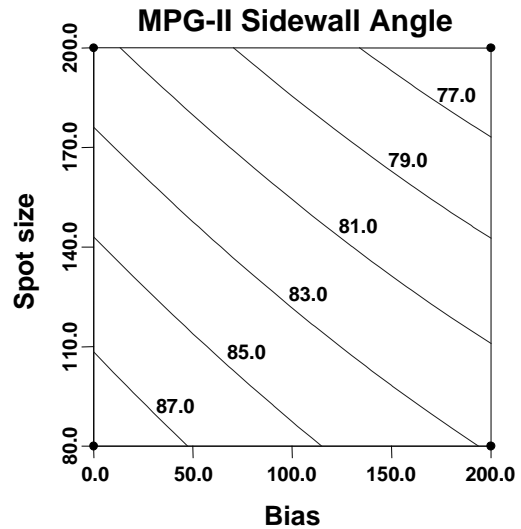


Figure 6. Sidewall angle as a function of spot size and bias — MPG-II, 5 nm input address, 164 sec development time.



5. EXPERIMENTAL PARAMETERS

Three 6-in. × 250-mil Ulcoat blanks coated with 4000 Å of ZEP 7000 were exposed on a 10 keV MEBES system. Each mask was exposed with the same pattern set, which included the full matrix of parameters: writing strategy, input address, data bias, development time, and spot size. Masks were exposed with the recommended parameters for a MEBES 5500, a 10 μC/cm² primary dose with a 4.1 μC GHOST dose and 900 nm GHOST spot. Masks were developed using ZED 750 developer. Each mask was developed for a unique length of time to span the entire parameter space. Development time was normalized, such that CD mean-to-target was minimized for the pattern exposed with MPG at a 30 nm input address and 160 nm spot size. After development, the masks were dry etched with a Plasma-Therm SLR-X, an inductively coupled system, using oxygen, chlorine, and helium gases.⁶ The etch consisted of a 60-sec oxygen descum, a bulk etch that was determined by endpoint, and a 90-sec overetch. The masks were then stripped and cleaned, and then measured on an automated, low-voltage KLA 8100ER CD-SEM. The landing energy used for measurement was 1000 eV, with a 20 pA beam current. A derivative algorithm was used for edge detection and CD measurement.

To improve the accuracy of the tests, each input permutation was written and measured eight times. An average of the eight measurements was used for the analysis. The area fill was calculated based on measurements of the KLA 8100 automated area, x-axis CD, and y-axis CD. The area of a contact was determined by fitting a 64-sided polygon to the contact feature. The area of the polygon is calculated and compared to the measured x and y CDs to determine the percentage of area fill. See Equation 1, area fill calculation, for a mathematical description of the area fill calculation.

$$\text{Area fill (\%)} = \frac{\text{Measured area (nm}^2\text{)}}{\text{Measured X (nm)} * \text{Measured Y (nm)}} * 100 = \frac{\text{Measured area (nm}^2\text{)}}{\text{Nominal area (nm}^2\text{)}} * 100 \quad (1)$$

6. EXPERIMENTAL RESULTS

Figures 7 and 8 show the experimental CD mean-to-target responses for MPG and MPG-II, respectively. The responses for the two writing strategies are almost identical. As expected, development time and bias show the largest impact. The development time response shows roughly a 2 nm CD change/sec development rate. The slope of the spot size response is larger for MPG; this is due in part to the larger range of spot sizes used in the experiment.

Figure 7. CD mean-to-target (MTT) — MPG.

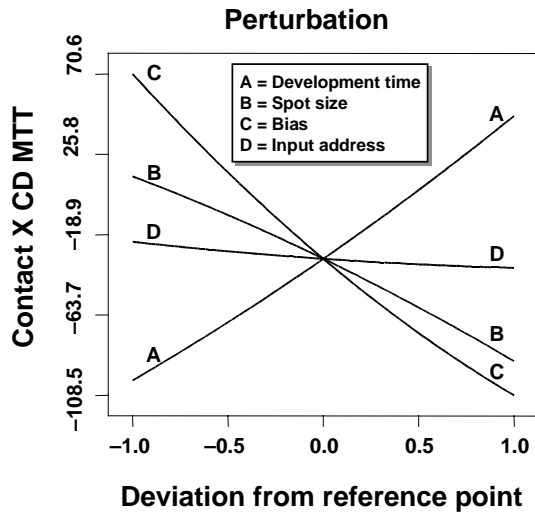
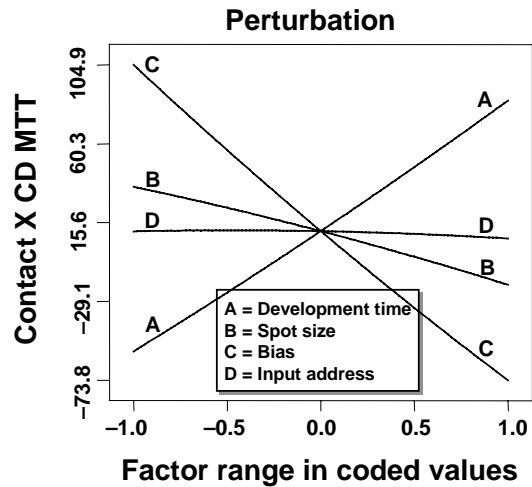


Figure 8. CD mean-to-target (MTT) — MPG-II.



The range in spot sizes for MPG is 160 nm, with a change in CD over that range of ~100 nm, whereas the change in CD for MPG-II is ~55 nm over a 120 nm spot size range. This implies that either the spot size response is nonlinear, or that not all of the difference in slope can be assigned to the spot size range difference. To better understand the difference, examine Figures 9 and 10, which are contour plots of CD mean-to-target as a function of input address and spot size for each strategy. Compare the change in CD at the 15 nm input address for both plots over the same spot size range (see highlighted area in Figure 9). The two responses show roughly the same range in CD, although an offset is apparent. The contours converge as the input address increases, such that the increase in sensitivity to spot size for MPG appears to be related to the larger input addresses. As the pixel size becomes a larger percentage of the final CD, more of an effect on CD would be expected.

Figure 9. CD mean-to-target (MTT) as a function of spot size — MPG, bias = 90 nm, development time = 240 sec.

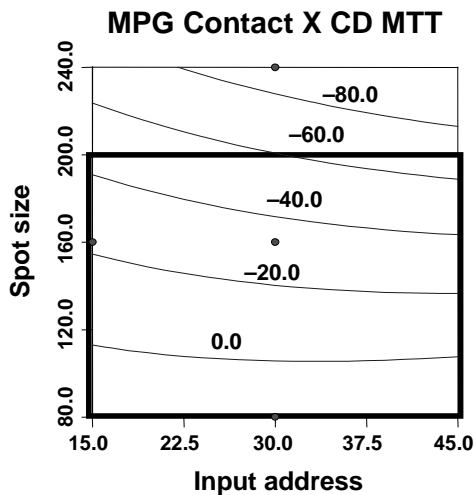
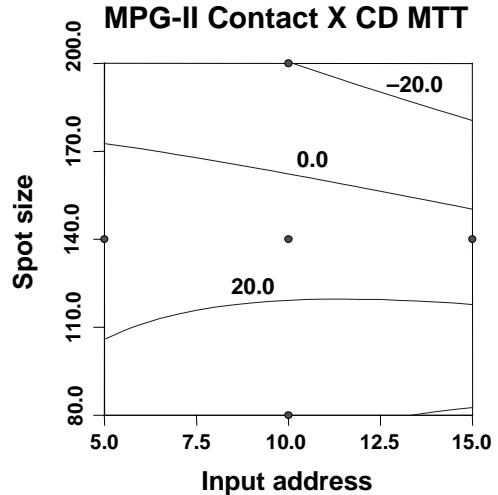


Figure 10. CD mean-to-target (MTT) as a function of spot size — MPG-II, bias = 90 nm, development time = 240 sec.



In addition to CD mean-to-target, the other response studied in the experiment was the contact area fill. Figures 11 and 12 show the area fill responses for each writing strategy. Both MPG and MPG-II show a degradation in area fill as the spot size increases. This is not independent of the CD mean-to-target, however, which is discussed later in this section. Both strategies also show a downward trend in area fill with bias and development time, with MPG-II showing a higher sensitivity to development time. Also notable is a slight increase in the maximum and minimum area fill for MPG-II as compared with MPG.

Figure 11. Area fill — MPG.

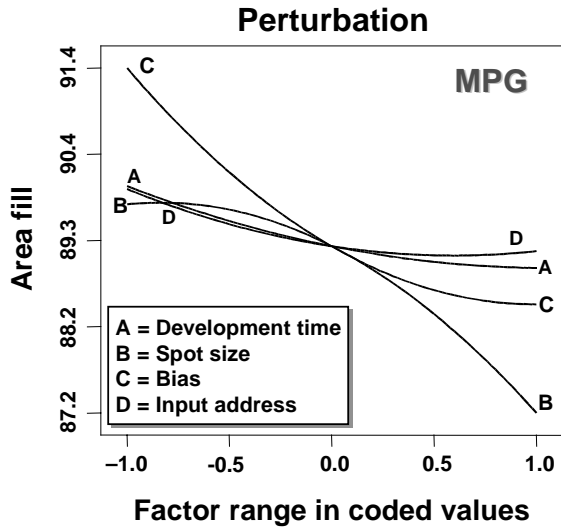
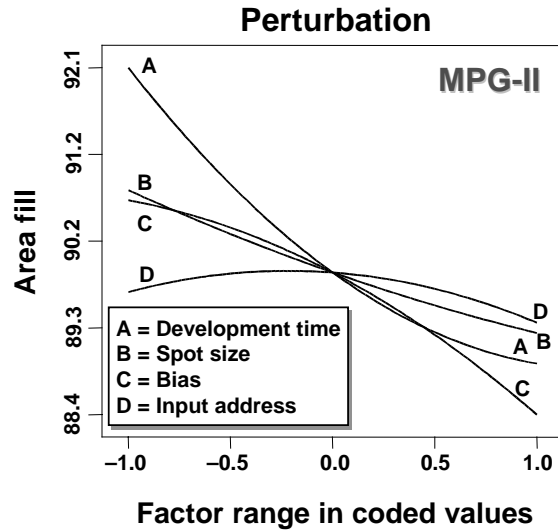


Figure 12. Area fill — MPG-II.



The impact of spot size on area fill is tied to the CD mean-to-target. We have already noted a decrease in CD with increasing spot size (Figures 7 and 8). There is an inherent dependence on CD to the area fill metric as well. For example, if we assume a constant area deficit, independent of CD, Equation 2 shows that the area fill will decrease as feature size is reduced. In other words, despite the quality of the feature being maintained, a degradation is perceived by the reduction in area fill. The perceived degradation is due to the fact that the constant area deficit is simply a larger fraction of the contact with smaller CDs. Even if the corner sharpness is being maintained such that the same amount of area is missing regardless of CD or spot size, we would see a decrease in area fill.

$$\text{Area fill (\%)} = \frac{\text{Measured area (nm}^2\text{)}}{\text{Nominal area (nm}^2\text{)}} * 100 = \frac{\text{Nominal area (nm}^2\text{)} - \text{Area deficit (nm}^2\text{)}}{\text{Nominal area (nm}^2\text{)}} * 100 = 1 - \frac{\text{Area deficit (nm}^2\text{)}}{\text{Nominal area (nm}^2\text{)}} * 100 \quad (2)$$

Suppose that the reduction in area fill observed in our analysis is entirely due to the CD change that occurs with spot size change, and that area deficit is constant regardless of CD or spot size. The area fill can be calculated for each contact and the results compared with the raw data. If the reduction in area fill is entirely due to the change in CD, the calculated area fill and raw area fill plots should overlay. Figure 13 shows the results of this analysis. The raw area fill and CD data shown are for MPG-II. The calculated area fill is the amount expected if we assume constant area deficit over the same range. The area fill is normalized to the first data point: the 80 nm spot size with the 5 nm input address.

The area deficit calculated from the raw data for the first data point was the constant area deficit for all subsequent points. What we find is that the calculated area fill and the raw area fill show the same trend, although they do not exactly match. This suggests that at least some of the source of the area fill degradation is related to CD, and some to the spot size itself.

Figure 14 includes SEM images that support these findings. Although feature quality degrades somewhat, the sensitivity to spot size is less than the initial analysis would suggest.

Figure 13. Area fill with a constant area deficit — MPG-II.

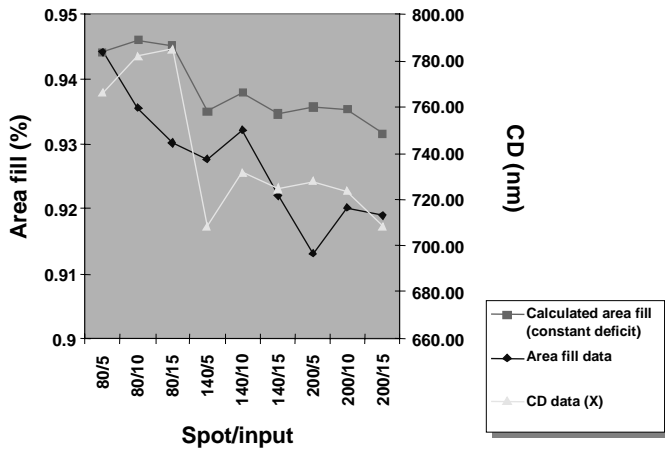
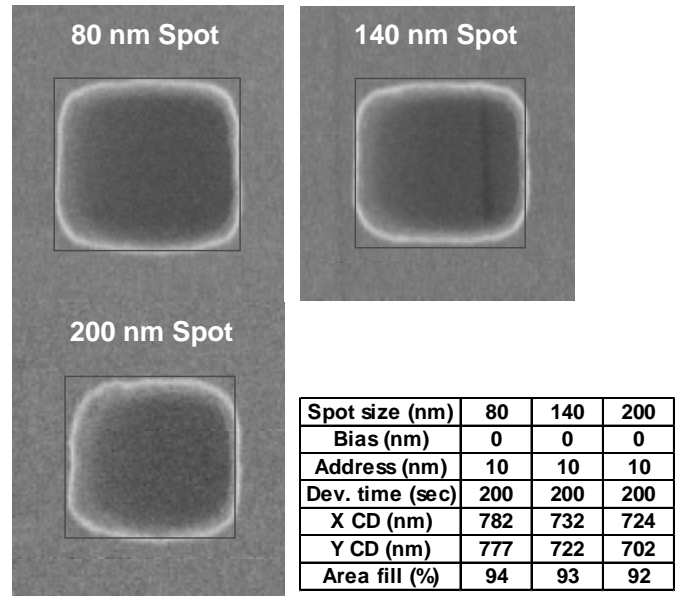


Figure 14. SEM images — varying spot/CD.



Additional SEM images were gathered to verify the area fill response to the other variables. Two cases are shown in Figures 15 and 16, the first to visually estimate the impact of development time on feature performance, and second to estimate the impact of bias. Figure 15 shows SEM images for a 720-nm design-size contact on two different masks. All SEM images were taken at the same magnification (100kX). The input address, bias, and spot size are fixed for these two images, and they are both exposed with MPG-II. Table 4 describes the process and exposure parameters, along with the measured CDs. Additional graphics are overlaid with the images to assist in a visual comparison between the two features. The images support the analysis: an increase in development time rounds the corners slightly and produces a lower area fill.

Figure 15a. 200 sec develop time.

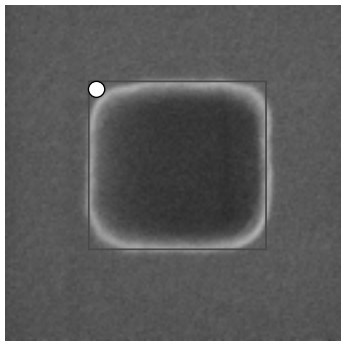


Figure 15b. 280 sec develop time.

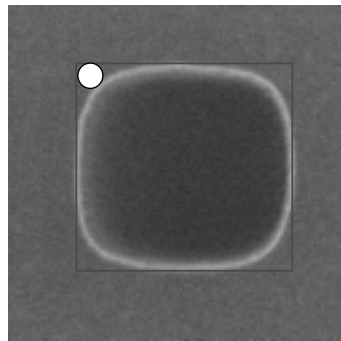
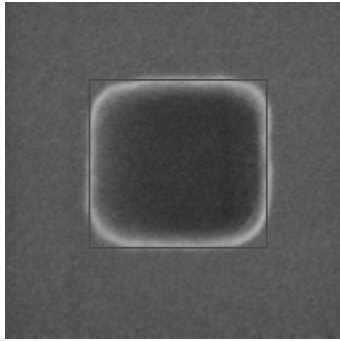


Table 4. CD and process.

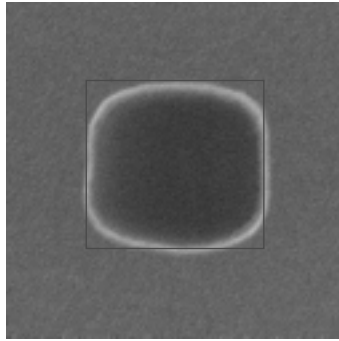
Parameter	Figure 15a	Figure 15b
Develop time (sec)	200	280
Writing strategy	MPG-II	MPG-II
Input address (nm)	10	10
Spot size (nm)	140	140
Bias (nm)	0	0
X CD (nm)	734	897
Y CD (nm)	711	878
Area fill (%)	94	90

This next set of SEM images shows the effect of bias on contact feature performance. The analysis indicates a reduction in area fill with increasing bias, and Figure 16 reflects this conclusion. Figure 16 shows images of the target CD for 0 bias, 90 nm bias, and 180 nm bias, respectively. The input address and spot size are fixed, and they are all exposed with MPG-II. They have different biases and, therefore, different development times to achieve the target CD. Table 5 describes their process and exposure parameters, along with the measured CDs. The impact of bias is coupled with the increase in development and shows similar results to the variable development time case shown in Figure 15. The contact feature becomes more rounded with bias, and a lower area fill is the result.

Figure 16a. 0 nm bias (200 sec develop).



b. 90 nm bias (240 sec develop).



c. 180 nm bias (280 sec develop).

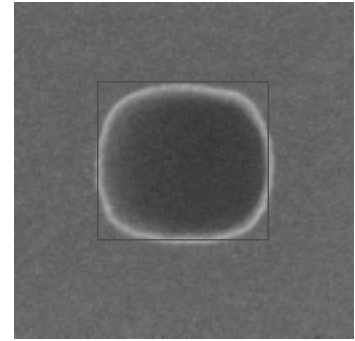


Table 5. CD and process.

Parameter	Figure 16a	Figure 16b	Figure 16c
Bias (nm)	0	90	180
Writing strategy	MPG-II	MPG-II	MPG-II
Input address (nm)	10	10	10
Spot size (nm)	140	140	140
Develop time (sec)	200	240	280
X CD (nm)	734	740	707
Y CD (nm)	711	722	674
Area fill (%)	94	90	87

The most significant influence on area fill of the tested parameters is bias, which also depends on the development time. Lower bias improves area fill performance. Although a reduction in area fill is observed relative to spot size, the CD dependence on spot size is an important factor to consider. The feature quality does not degrade with larger spot size as quickly as the initial set of data suggests, which emphasizes the importance of tracking CD and area fill simultaneously.

7. COMPARISON OF SIMULATION TO EXPERIMENT

One goal of this paper was to evaluate the efficacy of using simulation as a process development and characterization tool. Simulation can only be a useful tool if it can accurately predict experimental trends. If it is successful, then it can be used to help focus an experiment on the key variables, excluding the parameters that show little or no impact on the experiment. The payoff in coupling accurate simulation with experiment is a reduction in cost and time to achieve the overall goal. A strong correlation between simulation and experiment also increases the users' confidence in both methods.

CD mean-to-target results provide the overlap between simulation and experiment in this investigation of contact lithography. Area fill and sidewall profiles, the other responses to experiment and simulation, are not obviously linked and will not be discussed in this section. A worthwhile extension of this work to further test the correlation is to collect experimental cross-sectional data on sidewall profiles, as well as area fill calculations on 3D slices from simulation, but that work is beyond the scope of this paper.

Focusing on the CD mean-to-target response, Figures 17 and 18 show the MPG-II perturbation plots for simulation and experiment, respectively. The trends for all of the responses agree between simulation and experiment. A slight difference in the range of mean-to-target values is observed, which is likely due to the exclusion of the dry etch in the model. The correlation between simulation and experiment for MPG data is also strong, as seen in Figures 19 and 20. The increased sensitivity to spot size for MPG is observed in both the simulation and the experiment, although to a lesser extent in the simulation.

Figure 17. CD mean-to-target (MTT) — MPG-II simulation results.

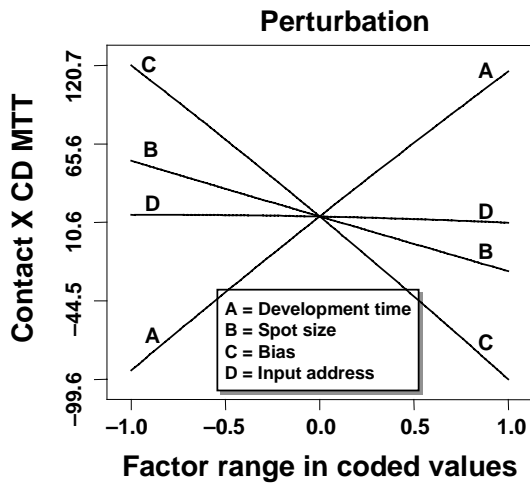


Figure 18. CD mean-to-target (MTT) — MPG-II experimental results.

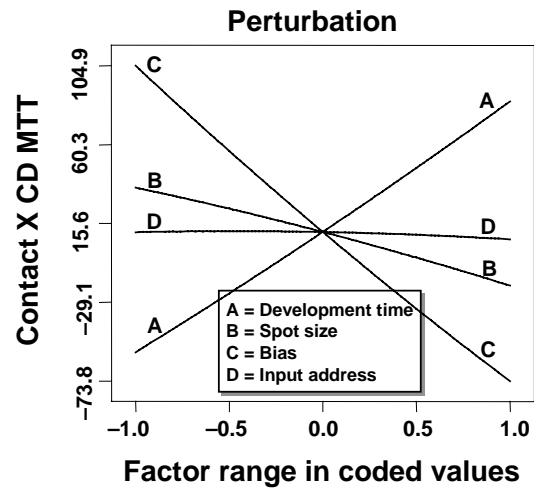


Figure 19. CD mean-to-target (MTT) — MPG simulation results.

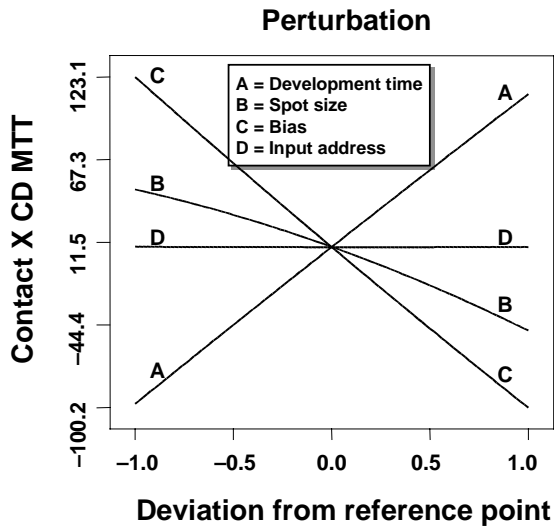
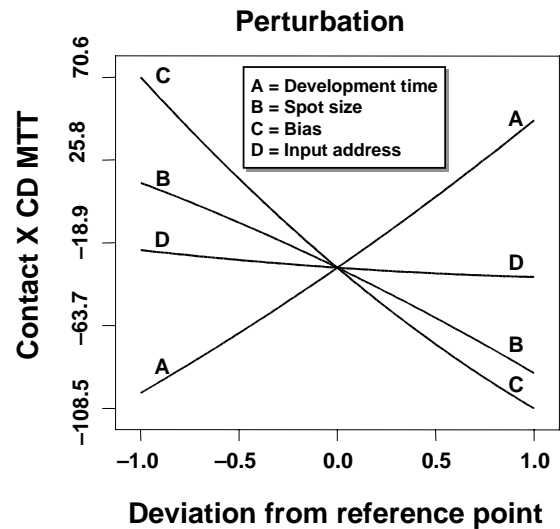


Figure 20. CD mean-to-target (MTT) — MPG experimental results.



8. CONCLUSIONS

One goal for this paper was to determine the optimum exposure and process parameters for contact features for MPG and MPG-II. The results indicate the following trends:

- $\Delta CD/\% \Delta dose$ is minimized for smaller spot sizes
- Sidewall angle is steeper for smaller spot sizes
- Input address has little influence on the CD mean-to-target and area fill responses
- As spot size increases, CD decreases, and correspondingly so does area fill
- Area fill and sidewall angle degrade with increasing development time and bias
- Contact lithographic performance is comparable for MPG and MPG-II writing strategies

The process window is determined by overlaying response solutions based on specified criteria. Figures 21 and 22 are overlay plots of MPG-II experimental data for two arbitrary criteria. The highlighted area is the region where the criteria are met, and defines the process window. There is no obvious improvement in the process window for increasing bias, as shown in Figure 21. Figure 22 shows that for a tighter area fill constraint, there is a limit to the amount of bias that can be applied.

Figure 21. Overlay 1. $-28\text{-nm} < CD$ mean-to-target, $<28\text{-nm}$ area fill, $>85\%$ MPG-II, 10 nm input address, 140 nm spot size.

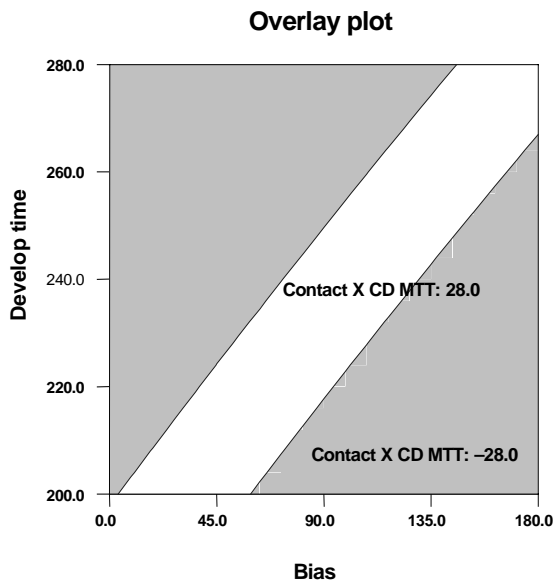
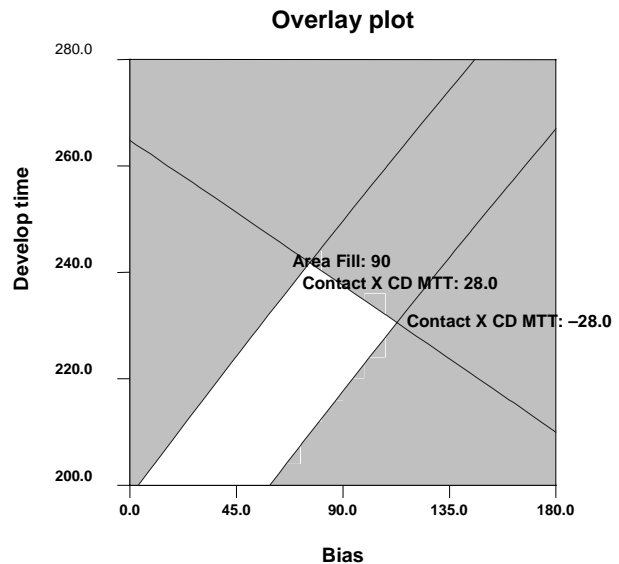


Figure 22. Overlay 2. $-10\text{-nm} < CD$ mean-to-target, $<10\text{-nm}$ area fill, $>90\%$ MPG-II, 10 nm input address, 140 nm spot size.



A second goal for the paper was to compare results from simulation and experiment to gauge the usefulness of using simulation as a process development and characterization tool. The results show a strong correlation between the experimental and simulated CD mean-to-target response for both writing strategies. Both methods show response insensitivity to input address and improvement in feature quality with smaller spot size and bias. The ranges in CDs and development times are roughly the same, the minor differences are attributed to exclusion of dry etch in the model, and small differences in the bias and development times between simulation and experiment. The positive correlation between simulation and experiment of the CD mean-to-target response encourages further correlation studies and the use of simulation as a process development and system characterization tool.

9. TRADEMARKS

MEBES and Etec are registered trademarks of Etec Systems, Inc., an Applied Materials Company. All other trademarks are the property of their respective owners.

10. REFERENCES

1. J. Chabala, S. Weaver, D. Alexander, H. Pierce-Percy, M. Lu, D. Cole, F. Abboud, "Evaluation of a High-dose, Extended Multipass Gray Writing System for 130-nm Pattern Generation," *SPIE Microlithography 2000*, Proceedings, to be published.
2. J. M. Chabala, et al, "Lithographic Analysis of Multipass Gray Writing Strategy for Electron-Beam Pattern Generation," *Emerging Lithographic Technologies III*, vol. **3676**, p. 80, 1999.
3. E. P. Box and N. Draper, "Empirical Model-Building and Response Surfaces," J. Wiley and Sons Inc. (New York: 1986), pp. 305–306.
4. C. A. Mack, "Three Dimensional Electron Beam Lithography Simulation," *Emerging Lithographic Technologies*, SPIE Proc., **3048**, pp. 76–88, 1997.
5. M. Lu, T. Coleman, and C. Sauer, "A 180 nm mask fabrication process using ZEP 7000, multipass gray, GHOST, and dry etch for MEBES 5000," *BACUS Symposium on Photomask Technology and Management*, vol. **3546**, p. 98, 1998.
6. B. Albrethsen-Keck, M. Lu, and C. Sauer, "Improving CDs on a MEBES system by improving the ZEP 7000 development and dry etch process," *BACUS Symposium on Photomask Technology and Management*, vol. **3873**, p. 592, 1999.
7. C. A. Mack, "Inside PROLITH, A Comprehensive Guide to Optical Lithography Simulation," FINLE Technologies (Austin, TX: 1997), pp. 106–110.
8. C. A. Mack, "Inside PROLITH, A Comprehensive Guide to Optical Lithography Simulation," FINLE Technologies (Austin, TX: 1997), p. 118.